

UC Berkeley

UC Berkeley Previously Published Works

Title

Recovery of dilute aqueous butanol by membrane vapor extraction with dodecane or mesitylene

Permalink

<https://escholarship.org/uc/item/05w5m5jj>

Authors

Chen, J
Razdan, N
Field, T
[et al.](#)

Publication Date

2017-04-01

DOI

10.1016/j.memsci.2017.01.018

Peer reviewed

Recovery of dilute aqueous butanol by membrane vapor extraction with dodecane or mesitylene

J. Chen^{a,b}, N. Razdan^a, T. Field^a, D.E. Liu^a, P. Wolski^a, X. Cao^b, J.M. Prausnitz^a, C.J. Radke^{a,*}

^a Chemical and Biomolecular Engineering Department, University of California, Berkeley, CA 94720, United States ^b State Key Laboratory of Bioreactor Engineering, East China University of Science and Technology, Shanghai 200237, China

* Correspondence to: Department of Chemical and Biomolecular Engineering, University of California, Berkeley, 101E Gilman Hall, Berkeley, CA 94720-1462, United States. E-mail address: radke@berkeley.edu (C.J. Radke).

Abstract

A novel, nearly isothermal, nonselective-membrane separation process, membrane vapor extraction (MVE), efficiently recovers butanol from a dilute aqueous solution, for example, from a fermentation broth (Liu et al., 2015). In MVE, feed and solvent liquids are not in contact; they are separated by vapor. Therefore, compared to conventional extraction, MVE avoids formation of difficult-to-separate emulsions.

In MVE, a semi-volatile aqueous solute (e.g., butanol) vaporizes at the upstream side of a membrane, diffuses as a vapor through the membrane pores, and subsequently condenses and dissolves into a high-boiling nonpolar solvent, favorable to the solute but not to water. Design analysis of a 1.5-m long, 30-m² membrane-area countercurrent MVE unit for processing 2-wt% aqueous butanol by dodecane solvent at 40 °C indicates over 90% recovery of the feed butanol with essentially no water loss and with very low energy requirement (Liu et al., 2015). The separation factor is over 1500. However, the published design study gives no experimental evidence for the calculated MVE separation.

Here, we present experimental data to validate the MVE process. We use an omniphobic (i.e., hydrophobic and oleophobic), 0.2- μm pore-diameter Versapor®200 R membrane (Pall Corporation, Exton, PA) housed in a 6-cm wide by 10-cm long plate-and-frame channeled flow cell with 0.8-cm gap thickness. Membrane transfer area is 28 cm². The membrane flow cell is designed for minimal axial concentration change and is operated in the transient mode between two recirculating flow loops.

2-wt% aqueous butanol is extracted into dodecane or mesitylene at 25 or 40 °C. Also, 1.5-wt% furfural is extracted into dodecane at 40 °C. Since vapor transport across the membrane contributes minimal resistance, MVE performance is governed by mass transfer through feed and solvent boundary layers. Mass-transfer coefficients are determined from the Graetz-Lévêque analysis of laminar thin-slit flow (Bird et al., 2002). Predicted extraction performance agrees well with experiment using no adjustable

parameters. Consistent with the initial multistage-design analysis (Liu et al., 2015), our new bench-scale experimental results confirm that MVE is a viable separation process to recover dilute semi-volatile biosolutes from water with minimal energy requirement. Preliminary analysis of downstream solute recovery from the extract via distillation is more efficient than that for pervaporation because of insignificant water carry over through the MVE membrane.

Keywords: Membrane vapor extraction, Mass-transfer resistance, Butanol or furfural recovery, Recirculation flow cell, Dodecane, Mesitylene

1. Introduction

Advances in biological engineering are increasing the number of biochemicals that can be produced by large-scale fermentation [3–5]. Potential fermentation products include the acetone-butanol-ethanol mixture, organic acids, hydrocarbon-fuel molecules, and light-organic building blocks [1]. Because the microbe-toxic concentration of bioproducts in an aqueous fermentation broth is typically below 5 wt% [4], these products must be recovered.

Current separation processes require high energy [6]. At present, recovery of fermentation bioproducts is commonly achieved by distillation. However, the high temperatures required for distillation of aqueous fermentation broths inhibit microbial growth and increase both energy requirements and operating costs [6]. Thus, alternative extraction processes are sometimes performed either prior to or instead of distillation. Recent developments in fermentation-product recovery suggest that membrane distillation (MD) may be a promising separation technique [7]. MD is a thermally-driven process where semi-volatile aqueous solutes in the upstream side vaporize across a microporous hydrophobic membrane to condense downstream [7]. The operating temperature and hydrostatic pressure in MD are low compared to those in distillation or reverse osmosis (RO) [1]. However, MD suffers from water carry-over and from low solute flux [7].

Nomenclature			
C_F	Mass concentration of solute in feed	x	Coordinate across thickness of membrane
C_{F0}	Initial mass concentration of solute in feed	z	Axial coordinate along the flow channel of MVE unit
C_S	Mass concentration of solute in solvent		
C_{S0}	Initial mass concentration of solute in solvent		
D	Solute binary diffusion coefficient in water		
k_m	Mass-transfer coefficient		
K	Partition coefficient= C_S/C_F		
L	Length of flow channel		
N	Mass flux of butanol		
Q	Volumetric flow rate of the stream		
V	Liquid volume		
v	Channel average flow velocity		
w	Width of the flow channel		
			<i>Greek symbols</i>
		α	= C_{S0}/C_{F0}
		δ	Gap thickness
		ν	= V_S/V_F
		τ	Solute residence time (Eq. (7))
			<i>Subscripts</i>
		F	Aqueous feed
		S	Solvent

To improve the selectivity of MD and to eliminate significant thermal loads, we recently proposed a novel membrane-based separation process,

membrane vapor extraction (MVE), where the downstream side is a nonvolatile receiving solvent that shows high affinity for the biosolute but not for water [1]. Consequently, transmembrane water flux is minimized. Unlike membrane liquid extraction (MLE) [8], the bioproduct in MVE fluxes through the membrane as a vapor, reducing transmembrane mass-transfer resistance [9]. MVE avoids solute concentration polarization. Relative to MD, there is no imposed transmembrane temperature or pressure difference. The only driving force in MVE is the solute chemical-potential difference between the feed (upstream) and the solvent (downstream) side of the nonpermselective membrane. In comparison to pervaporation, no imposed vacuum or vapor condensation is required in MVE [1]. Previous investigations have experimentally demonstrated that aqueous biosolutes can be extracted from solution using an essentially isothermal chemical-potential driving force, provided that solvent affinity for the bio-product is sufficiently large [10,11]. The receiving solvent in MVE must be essentially nonvolatile to ensure that minimal transmembrane vapor flux reaches the upstream side. The bioproduct can then be readily distilled from the nonvolatile solvent with essentially zero water loss. To assure that the membrane flux is a vapor, the membrane must be nonwetting to both water and the downstream organic solvent; for MVE, the membrane must be both hydrophobic and oleophobic. There is no need for membrane permselectivity as bulk phase equilibria set separation performance. Accordingly, membrane synthesis is not required for each new chemical separation, as in the various embodiments of pervaporation. A very important advantage of MVE is that the two liquid streams are never in contact, circumventing formation of difficult-to-separate emulsions frequently found in bioproduct liquid-liquid extraction [12].

Fig. 1 illustrates MVE for recovery of aqueous butanol. Butanol in the feed vaporizes into the omniphobic porous membrane, diffuses through the membrane pores, and dissolves into a nonvolatile solvent. There is almost no net temperature or pressure change along either the pore or axial length of the membrane and essentially no transfer of water into the downstream solvent. MVE allows continuous fermentation by maintaining the biosolute below toxic concentration and with little or no need for makeup water.

Previously, we presented an engineering analysis for a 1.5-m long, 30-m² membrane-area, countercurrent MVE unit for processing a 2-wt % aqueous butanol feed by a prototype solvent (dodecane) at 40 °C. The analysis showed over 90% recovery of the feed butanol with essentially no water loss. The separation factor was well over 1000. However, the initial design study gave no experimental evidence supporting MVE separation [1]. In this work, we provide laboratory validation of the MVE process. We focus on verifying MVE in a smallscale membrane module incorporated into circulating flow loops of feed and solvent, illustrated in Fig. 2. The laboratory-size unit operates in the unsteady-state mode towards equilibrium in contrast to the commercial-scale unit that operates in the steady-state, countercurrent mode [1]. Because the membrane-module in our laboratory experimental

study has a larger gap size, smaller length and flow rates, and most importantly, a membrane surface area 10^4 times smaller than that in the design study, observed final solute concentrations in the receiving solvent are not as large.

2. Experiment

2.1. Materials

The feed is an aqueous solution containing 2-wt% butanol (close to the current tolerance limit for biofuel microbes). As an alternate to butanol, 1.5-wt% aqueous furfural is the feed in one set of transient MVE experiments. Like butanol, furfural is a useful bio-based product [13]. Dodecane or mesitylene are the extracting solvents. Butanol-1 was purchased from Alfa Aesar (Tewksbury, MA); furfural was obtained from Sigma Aldrich (St Louis, MO); dodecane was from TGI (Portland, OR); and mesitylene was from Spectrum Chemical (Gardena, CA), all with 99% purity and used as received. Domestic water was purified sequentially by carbon filtration, reverse osmosis, and UV exposure to a resistivity of 18 M Ω .

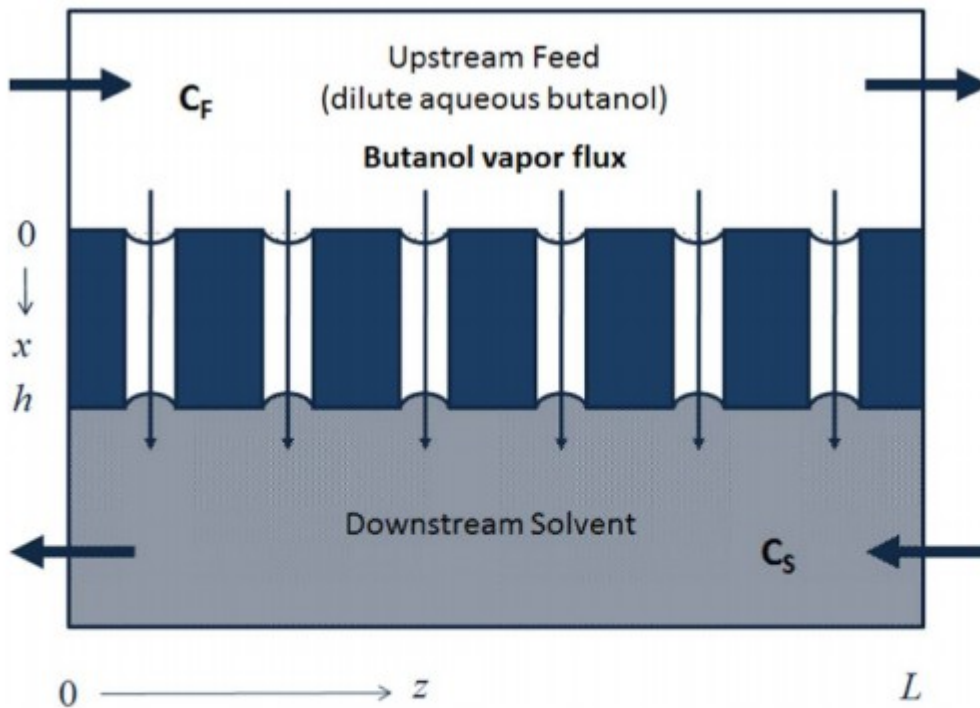


Fig. 1. Schematic of a countercurrent MVE module. Upstream feed is shown in white; the omniphobic, microporous membrane is shown in dark shading; the downstream solvent is shown in intermediate gray. Butanol in the aqueous feed vaporizes, diffuses through the pores, and absorbs into the solvent. The concave curvature of the nonwetting pore menisci and contact-line pinning at the pore mouths prevent liquid entry at each end of the pore.

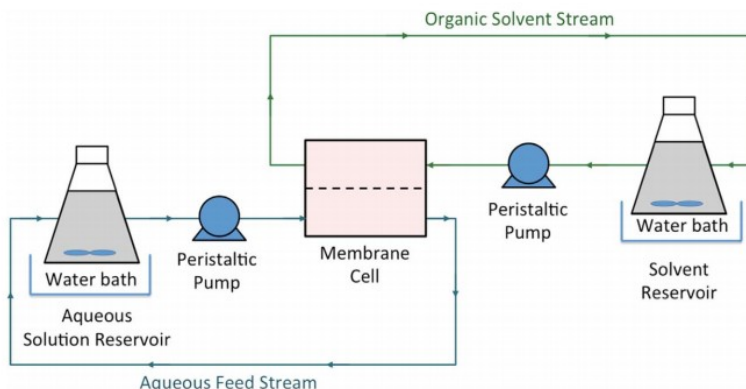


Fig. 2. Schematic of MVE module and flow loops. Aqueous feed and organic solvent streams recirculate through the membrane module to their respective thermostatted reservoirs. Transient solute concentrations are measured by sampling from the reservoirs.

Table 1 gives details for the Versapor®200 R membranes (Pall Corporation, Exton, PA [14]). Membranes are composite acryliccopolymer surface-layers covering a nonwoven nylon core. They are 150–300 μm in total thickness and are treated by a Repel™ surface coating to be nonwetting to water and to most organic solvents [14]. The 0.2- μm pore diameter is small enough to withstand large capillaryentry pressures (e.g., 1 bar for water), but large enough to support significant vapor transport.

2.2. Analytical methods

Butanol and furfural concentrations in the aqueous feed were measured using HPLC (LC-20AD, Shimadzu, Kyoto, Japan) after calibration with known solute-concentration standards. 10- μL aliquots were injected onto a Phenomenex Rexex RFQ-Fast Acid H+ column (100 \times 7.8 mm; mobile phase: 0.01 N H_2SO_4 ; flow rate: 1.0 mL/min; temperature: 30 $^\circ\text{C}$ for butanol and 55 $^\circ\text{C}$ for furfural).

Butanol and furfural concentrations in the solvent were measured by gas chromatography (Varian CP-3800, Palo Alto, CA) equipped with a Factor Four capillary column (UF-5 ms 30 m, 0.25 mm, 0.25 μm , P/ N CP8944) connected to a flame-ionization detector and pre-calibrated with known concentration solute/solvent standards.

To check for possible water carry-over into the solvent stream during MVE, water content of downstream solvent at the end of several flow experiments was measured by Karl Fischer titration (Titrand 851, Metrohm, Herisau, CH).

2.3. Liquid-liquid equilibria

To ensure that dodecane and mesitylene are appropriate solvents for separation of butanol from water, and to minimize adjustable model parameters, independent liquid-liquid equilibria (LLE) experiments were performed. 10 mL of a 2-wt% butanol or 1.5-wt% furfural aqueous solution was contacted with 10 mL of solvent in glass vials. Vials were placed in 25 or 40 $^\circ\text{C}$ water bath over a 24-h period, intermittently shaken, and allowed to settle. Final equilibrium solute concentrations were ascertained by liquid

chromatography for the aqueous solutions and by gas chromatography for the solvent phases. Table 2 reports measured butanol partition coefficients in the two solvents, $K = C_S/C_F$, where C is the mass concentration of butanol or furfural and subscripts S and F indicate solvent (dodecane or mesitylene) and feed (aqueous solution), respectively. The partition coefficient for aqueous furfural in dodecane at a 40 °C is 0.40. Because the solutes are dilute and concentration changes are not large, we approximate K as a function of temperature only, assuming that the change in the ratio of solute activity coefficients with concentration in the feed and solvents is minimal. For both solvents, butanol and furfural prefer water. Partition coefficients of butanol are larger for mesitylene than for dodecane; they rise with increasing temperature. The partition coefficient of aqueous furfural in dodecane is larger than that for butanol.

2.4. MVE membrane module

The laboratory-scale plate-and-frame membrane module, illustrated in Fig. 3, minimizes mass-transfer resistances in the feed and solvent streams, displays minimal residence time compared to that in the recirculating flow loops, exhibits minimal concentration change in the channel axial direction, and provides measureable feed and solvent reservoir-concentration changes over a convenient laboratory time frames. Channel flow width $w=4$ cm and length $L=7$ cm, giving a membrane transfer area of 28 cm².

Under laminar-parabolic flow, the length-averaged mass-transfer coefficient obeys the theory of Graetz and L ev eque [1,2]:

$$\frac{k_m \delta}{D} = 2.935 \left(\frac{Q \delta}{w L D} \right)^{1/3} \quad (1)$$

where k_m is the mass-transfer coefficient, δ is the channel gap thickness, D is the solute binary diffusion coefficient in water at 40 °C (i.e., 1.2×10^{-5} cm²/s for butanol [15] and 5×10^{-6} cm²/s for furfural [16]), and Q is the volumetric flow rate, equal in both channels. Eq. (1) indicates that larger mass-transfer coefficients arise for small gap thicknesses. Physical limitations set the gap thickness in each flow channel at 0.78 cm. For the flow rates studied, 40 mL/min and 120 mL/min, average axial velocities are a near 20 cm/min giving Reynolds numbers less than 0.5 and mass-transfer coefficients in the feed stream of approximately 5×10^{-4} cm/s for butanol and 3×10^{-4} cm/s for furfural. Because the physical properties of the aqueous and solvent streams are similar, we equate mass-transfer coefficients in both feed and solvent streams.

Table 1

Versapor®200 R membrane properties [14].

Supplier	Pall Corporation
Material	Acrylic copolymer
Thickness	150–300 μm
Pore size	0.2 μm
Water breakthrough pressure	> 1.75 bar
^a Contact angle of water	128 \pm 3°
^a Contact angle of dodecane	108 \pm 5°
^a Contact angle of mesitylene	100 \pm 7°

^a measured advancing angles.

Fig. 3a shows the membrane module while Fig. 3b gives a schematic of one of the rectangular flow channels. The module consists of four Teflon® blocks each 6-cm wide, 10-cm long, and 0.5-cm thick, sealed against each other by O-rings and 6 through-bolts. The innermost two blocks sandwich the membrane. Flow visualization is important to confirm lack of air bubbles during filling and the lack of membrane liquid-phase cross-over of either feed or solvent streams. Therefore, 1-cm thick plate-glass windows are installed in the two outside block faces. At the inlet and outlet of each channel, machined shelves distribute the flowing liquid evenly over the entire width of the channels validating use of Eq. (1). Inlet and outlet ports consist of 1/4-in threaded cylindrical holes allowing connection to 1/8-in diameter PTFE tubing.

Table 2

Partition coefficients of butanol at 25 and 40 °C.

Solvent	Temperature °C	$K (=C_S/C_F)$
Dodecane	25	0.13
	40	0.22
Mesitylene	25	0.55
	40	0.83

2.5. MVE flow loops

As shown in Fig. 2, two separate flow loops recirculate feed and solvent to and from well-stirred reservoirs, each 250 mL and immersed in separate temperature-controlled water baths. Fluid transfer is via two peristaltic pumps (Masterflex 07553-70 and 07520-40 ColeParmer LLC, Court Vernon Hills, IL) at equal volumetric flow rates. The circulation direction of the feed stream is opposite to that of the solvent stream, although flow direction is

immaterial because concentration changes along the membrane module are minimal. To maintain constant temperature, all flow lines were insulated (Silicone Insulating Tape, Z175633-1EA, Sigma Aldrich, St. Louis, MO). Intermittently, 0.5-mL aliquots were withdrawn from each reservoir and analyzed for the concentration of butanol or furfural by chromatography.

Transient MVE experiments were conducted with 100 g of 2-wt% aqueous butanol or 1.5-wt% furfural transferring into 100 g of solvent. Feed and solvent transient butanol concentrations were obtained at two temperatures (25 or 40 °C) and at two flow rates (40 or 120 mL/ min). For mesitylene at 40 °C, the temperature of the downstream solvent was set slightly above that of the upstream feed to prevent condensation of water.

2.6. Membrane omniphobicity

To confirm membrane omniphobicity, captive-drop-advancing contact angles for the feed and solvent liquids were measured using dropshape analysis [17] on a commercial contact-angle goniometer (Krüss, DSA1, Charlotte, NC). Resulting angles are listed in Table 1. With a 0.2- μm pore diameter and with the contact angles in Table 1, YoungLaplace theory predicts capillary-entry pressures of approximately 1 bar for water and for dodecane. For mesitylene, the predicted entry pressure is closer to 0.1 bar. In our experiments, these capillary-entry pressures prevent feed and solvent invasion into the membrane pores.

MVE demands that capillary-entry pressures are not exceeded across the membrane, especially during filling. To ensure no membrane-liquid cross-over, we flowed water in both channels with one stream laced with 2-wt% butanol and 0.01-wt% sodium fluorescein dye (Sigma-Aldrich, F-6377-100G, Sigma-Aldrich, St. Louis, MO). The dye-free channel stream was observed visually for possible dye appearance during filling and subsequent steady flow for 8 h. The identical procedure was used for dodecane and mesitylene solvents, one stream containing 1-wt% butanol and 0.01- wt% Red IK oil-soluble dye (D53004, Chromatech Canton, MI). In all cases, no dye was observed in the undyed channel liquid. This observation along with excellent agreement of experiment with theory using no adjustable parameters validates the essential feature of the MVE process that only vapor transports across an omniphobic membrane.

Visual dye experiments also confirmed parabolic flow profiles in each channel with minimal entrance and exit effects. This result substantiates Eq. (1) to predict mass-transfer resistance.

3. Theory

3.1. MVE solute flux

Transport of a solute from the aqueous feed into the solvent by MVE consists of convective-diffusion from the feed to the membrane, feed-side evaporation of the solute, convective-diffusion of solute in the vapor phase

through membrane pores, dissolution of solute into the solvent phase, and convective-diffusion into the solvent stream. A major advantage of MVE is that the transport resistance in the gas phase of the membrane pores is negligible [1]. Consequently, the overall mass-transfer resistance in MVE is equivalent to that in liquid/ liquid extraction. Thus, the inverse overall mass-transfer coefficient is given by $k_{mF}^{-1} + (Kk_{mS})^{-1}$ where K is the equilibrium partition coefficient and k_m is a concentration-based mass-transfer coefficient [1,2]. Estimation of the mass-transfer coefficients k_{mF} and k_{mS} is a priori from Eq. (1) [1,2]. We find that feed and solvent mass-transfer coefficients are essentially the same. Accordingly, the mass flux, N , of solute through the membrane is given by

$$N = \frac{k_m}{(1 + K^{-1})} (C_F - C_S/K) \quad (2)$$

Large mass-transfer and partition coefficients improve MVE solute fluxes.

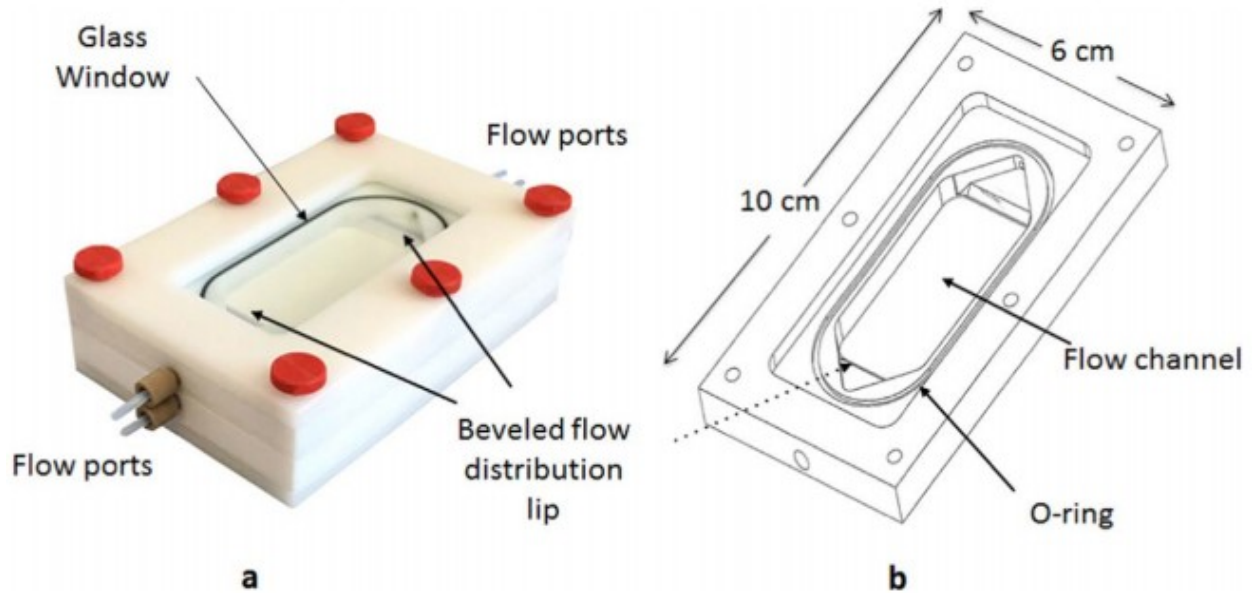


Fig. 3. Membrane module. (a) photograph (b) schematic of top flow channel.

We design the laboratory membrane module and flow loops such that the residence time in the membrane module is much less than those in the feed and solvent vessels or $wL^2/V \ll 1$ where V is the volume of liquid in the feed or solvent vessel (see Fig. 2). The membrane module exhibits minimal axial concentration changes when $wk_mL/Q \ll 1$. Under these conditions and upon neglect of residence time in the flow lines, solute mass balance of solute over the feed and solvent vessels are, respectively,

$$V_F \frac{dC_F}{dt} = -wLN \quad (3)$$

and

$$V_S \frac{dC_S}{dt} = wLN \quad (4)$$

Integration of Eqs. (2)–(4) is straightforward. Let the initial concentrations of butanol in the feed and solvents streams be designated C_{F0} and C_{S0} , respectively. We then find that

$$\frac{C_F}{C_{F0}} = \frac{1 + \alpha\nu + \nu[K - \alpha]\exp(-t/\tau)}{1 + K\nu} \quad (5)$$

and

$$\frac{C_S}{C_{F0}} = \alpha + \frac{(K - \alpha)}{1 + K\nu} [1 - \exp(-t/\tau)] \quad (6)$$

where $\alpha = C_{S0}/C_{F0}$, $\nu = V_S/V_F$, and the solute residence time in the flow loops is

$$\tau = \frac{V_S(1 + K)}{k_m wL(1 + K\nu)} \quad (7)$$

Apparatus design sets a convenient measurement time of $3\tau \sim 7$ h. Since all physical parameters are known, Eqs. (5)–(7) permit a priori calculation of the measured concentrations of butanol in the feed and solvent vessels.

4. Results

To provide experimental validation of the MVE process, we first conducted MVE experiments with 2-wt% aqueous butanol extracted into dodecane. Fig. 4 shows typical butanol concentration histories in the feed and solvent reservoirs at 40 °C and a flow rate of 40 mL/min ($v=12.8$ cm/min average velocity). Filled circles illustrate measured butanol concentration depletion from the aqueous feed stream, whereas open triangles demonstrate absorption of butanol into the countercurrent dodecane solvent stream. Standard-deviation error bars are shown in Fig. 4, and in those to follow, for three repeat experiments. Solid and dashed lines represent a priori prediction from theory (Eqs. (5)–(7)) using mass-transfer coefficients from the GraetzLévêque analysis for laminar channel flow ($k_m=5.2 \times 10^{-4}$ cm/s) and the measured equilibrium partition coefficient in Table 2. Excellent agreement is achieved including the final equilibrated concentrations. This result, along with the lack of dye cross-over in Section 2.6, confirm that butanol transport through the omniphobic membrane is via the vapor phase

only with negligible mass-transfer resistance. Fig. 4 validates the MVE process [1].

Fig. 5 displays as filled squares measured transient butanol flux corresponding to the experiments in Fig. 4. The experimental flux was determined from measured feed and solvent-reservoir concentration changes over a 1 h interval using Eqs. (3) and (4). Flux from the feed side estimated from Eq. (3) was identical to that into the solvent side from Eq. (4) within experimental error. The average of those two values is reported as filled squares in Fig. 5. The solid line gives the theoretical prediction from Eqs. (2) and (5)–(7), again using no adjustable parameters. Butanol MVE flux is largest at initial time and decreases monotonically to zero when liquid/liquid phase equilibrium emerges. Experimentally determined butanol flux is in excellent agreement with the a priori theoretical prediction. Overall mass balance for butanol or furfural is always closed to within experimental error.

The maximum measured flux in Fig. 5 is 1.8×10^{-6} g/cm²/s (0.065 kg/m²/h). Under identical initial feed and solvent compositions, butanol flux in the engineering-design analysis is 0.45 kg/m²/h [1], about seven times larger than that in our laboratory MVE module. Differences in phase-equilibrated compositions, flow rates, and channel dimensions (i.e., channel gaps, widths, and lengths) explain the lack of agreement. Also, the industrial-scale design utilized mass-transfer coefficients corresponding to plug flow through a slit filled with woven spacer [1], whereas our laboratory membrane module corresponds to parabolic flow through an open slit.

Reported flux for recovery of 2-wt% aqueous butanol with a highly selective pervaporation membrane (Hydrophobic HybSi@) is 0.5 kg/m²/h [18] close to that in our industrial-scale design [1]. Separation factors for the unsteady laboratory MVE system do not directly correspond to those for a steady process unit. If we define an equilibrium separation factor by the ratio of butanol to water concentration in the equilibrated extract divided by that ratio in the equilibrated raffinate, we find values again near 1500, comparable to that in the steady-state design unit and much larger than those in pervaporation of 10–100 [18]. Our proposed MVE process demonstrates essentially no water carry-over giving separation factors almost two orders of magnitude larger than those for pervaporation [1] and with no need for costly vacuum.

To provide additional support for the MVE process, we varied operating temperatures, flow rates, and receiving solvents. Figs. 6 and 7 show transient butanol concentration histories in the aqueous feed (filled circles) and dodecane solvent (open triangles) streams at ambient temperature and at 120 mL/min flow ($v=38.5$ cm/min), respectively. Lowering the temperature from 40 to 25 °C lowers the saturation concentration of butanol in the downstream dodecane from 0.46 to 0.32 wt%, as confirmed by the LLE data in Table 2. Increasing the flow rate by a factor of 3 has a barely

perceptible effect due to the insensitivity of the mass-transfer coefficients to flow velocity. Again, solid and dashed lines represent theory using the measured temperature dependence of the partition coefficients in Table 2 and temperature-independent mass-transfer coefficients from Graetz-Lévêque. Both figures highlight excellent agreement between experiment and theory using no adjustable parameters.

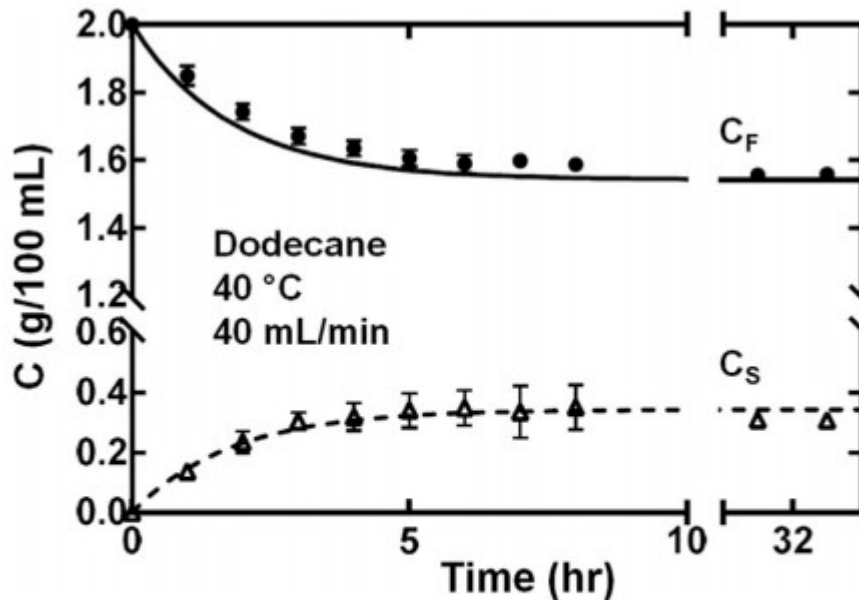


Fig. 4. Butanol concentration histories at 40 °C and $v=12.8$ cm/min. Filled circles and open triangles represent experimental data for aqueous feed and dodecane solvent, respectively. Solid and dashed lines give *a priori* theoretical prediction of feed and solvent butanol concentrations, respectively. Error bars represent standard deviation in three repeat experiments.

Figs. 8 and 9 report the role of mesitylene solvent in MVE recovery of dilute butanol from water. Since the partition coefficients of butanol in water towards mesitylene are larger than those toward dodecane, the downstream butanol saturation concentration and overall driving force are larger, nearly doubling the butanol saturation concentration from 0.46 to 0.84 wt% at 40 °C. Changing temperature with mesitylene gives the same trend as that for dodecane. Increasing temperature, increases the partition coefficient resulting in larger extraction efficiency. Comparison between a priori theory and experiment shows about 10% deviation. However, because experimental data error is $\approx \pm 7\%$, the experimental data are in good agreement with prediction.

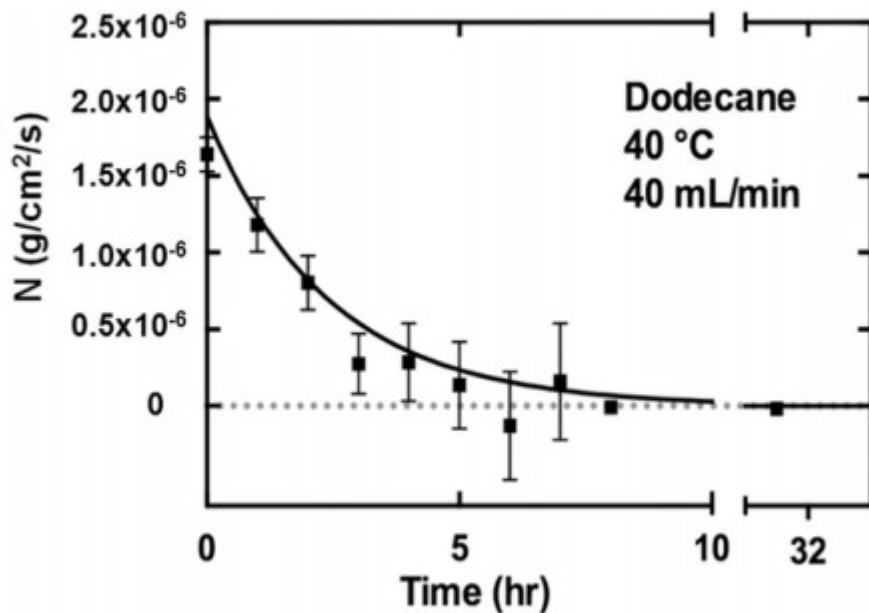


Fig. 5. Butanol flux history. Filled squares are experimental data; the solid line is *a priori* theory. Error bars represent standard deviation in three repeat experiments.

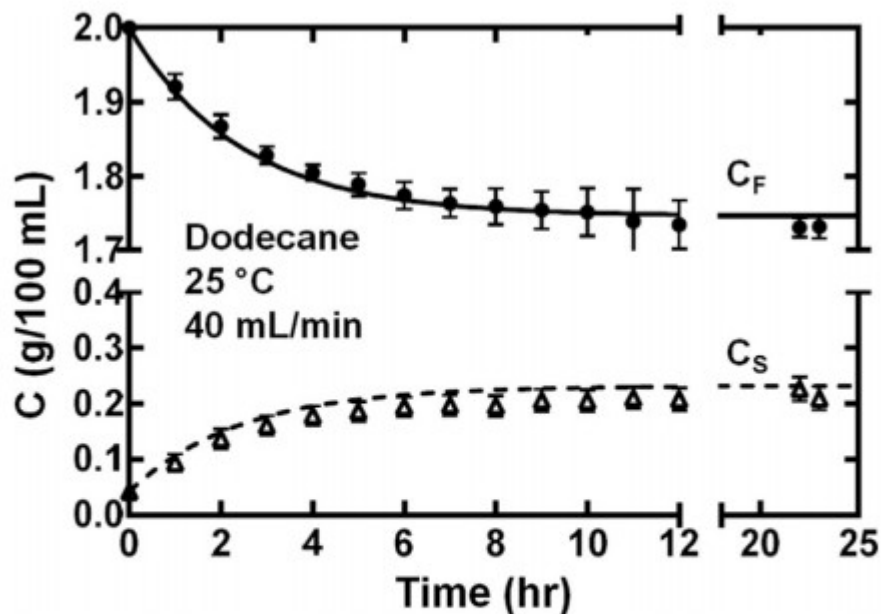


Fig. 6. Butanol concentration histories at 25 °C and $v=12.8$ cm/min. Filled circles and open triangles represent experimental data for aqueous feed and dodecane solvent, respectively. Solid and dashed lines give *a priori* theoretical prediction of feed and solvent butanol concentrations, respectively. Error bars represent standard deviation in three repeat experiments.

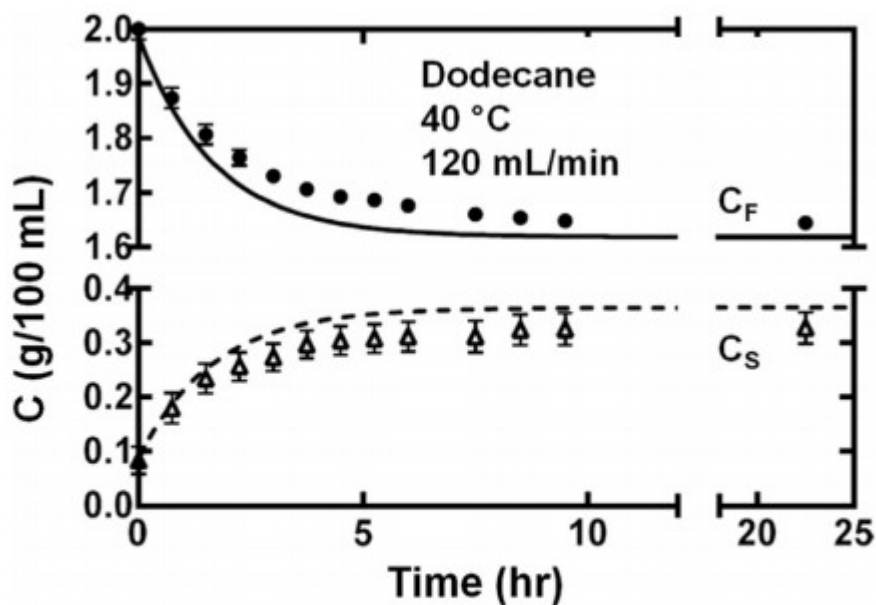


Fig. 7. Butanol concentration histories at 40 °C and $v=38.5$ cm/min. Filled circles and open triangles represent experimental data for aqueous feed and dodecane solvent, respectively. Solid and dashed lines give *a priori* theoretical prediction of feed and solvent butanol concentrations, respectively. Error bars represent standard deviation in three repeat experiments.

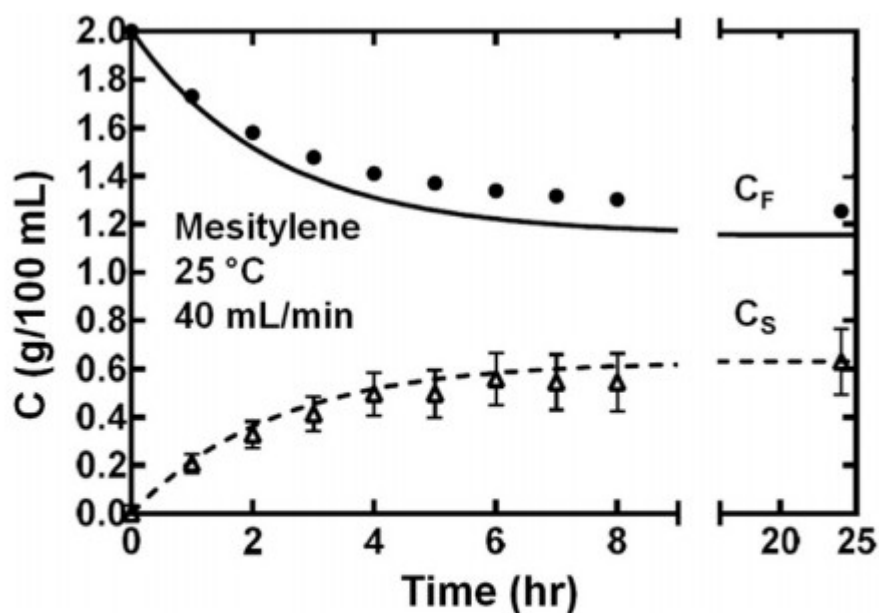


Fig. 8. Butanol concentration histories at 25 °C and $v=12.8$ cm/min. Filled circles and open triangles represent experimental data for aqueous feed and dodecane solvent, respectively. Solid and dashed lines give *a priori* theoretical prediction of feed and solvent butanol concentrations, respectively. Error bars represent standard deviation in three repeat experiments.

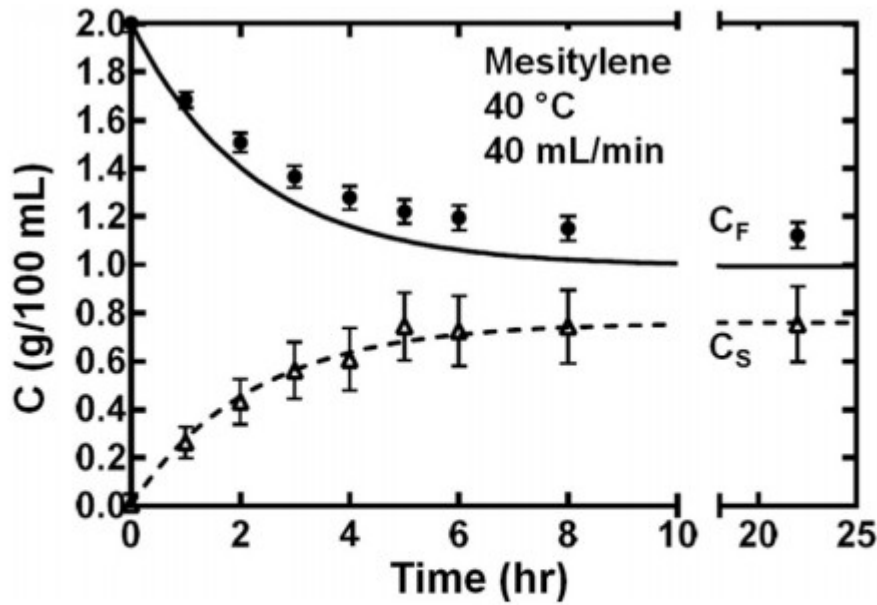


Fig. 9. Butanol concentration histories at 40 °C and $v=12.8$ cm/min. Filled circles and open triangles represent experimental data for aqueous feed and mesitylene solvent, respectively. Solid and dashed lines give *a priori* theoretical prediction of feed and solvent butanol concentrations, respectively. Error bars represent standard deviation in three repeat experiments.

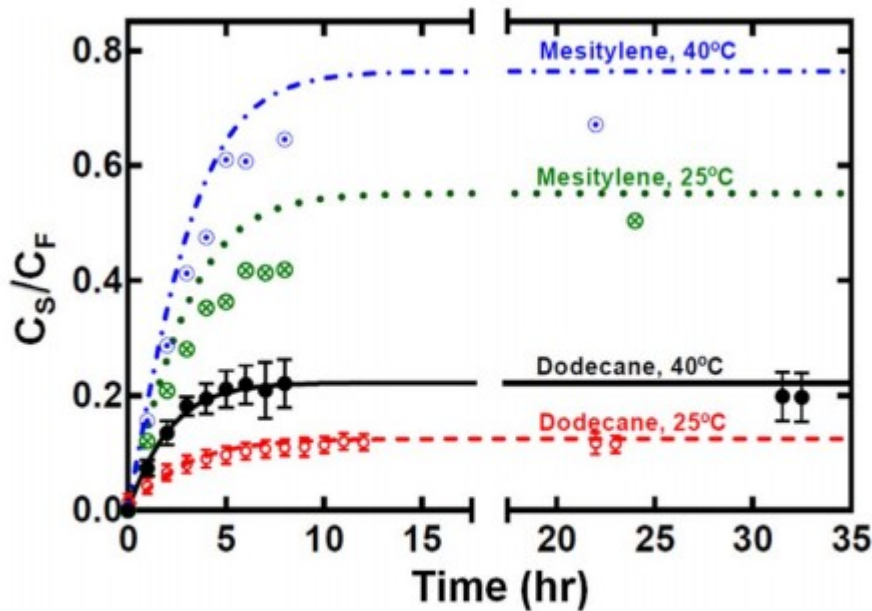


Fig. 10. Transient butanol solvent/feed partition ratio at 25 and 40 °C in dodecane or mesitylene solvents. Circles correspond to experiment. Lines represent *a priori* theory. Error bars represent standard deviation in three repeat experiments.

A strong test of the MVE process is to compare the measured transient partition ratio C_S/C_F against theory. Fig. 10 shows this comparison for butanol

with both solvents and operating temperatures and flows. Again, the experimental data show excellent agreement with the theoretical predictions. At 25 °C, the equilibrium ratio of butanol in the solvent and feed side is appreciably smaller than that at 40 °C. Changing the receiving solvent from dodecane to mesitylene, however, has a more drastic effect, tripling butanol recovery. Figs. 4–10 provide strong evidence validating MVE separation.

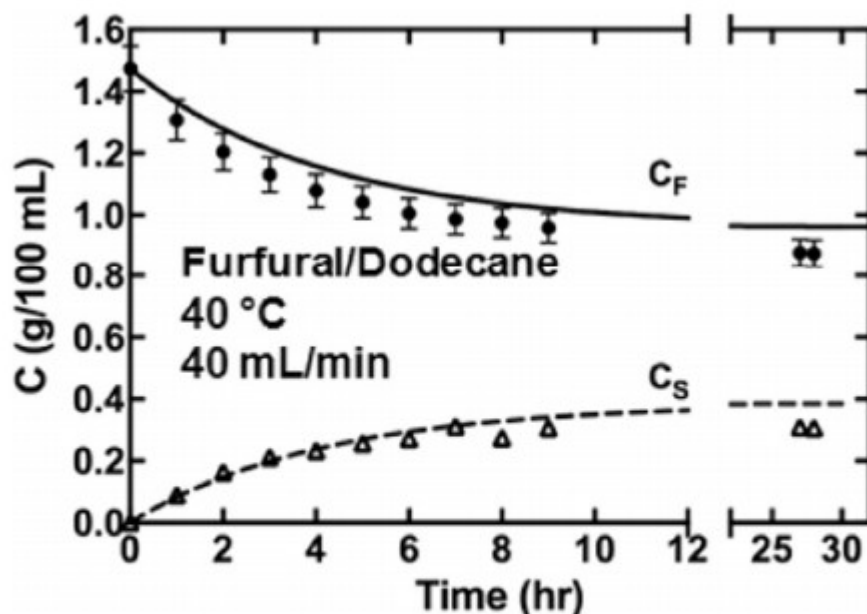


Fig. 11. Furfural concentration histories at 40 °C and $v=12.8$ cm/min. Filled circles and open triangles represent experimental data for aqueous feed and dodecane solvent, respectively. Solid and dashed lines give *a priori* theoretical prediction of feed and solvent butanol concentrations, respectively. Error bars, evident when larger than symbol size, represent standard deviation in three repeat experiments.

Table 3

Final water content in the solvent reservoir of the MVE apparatus.

MVE solvent	water content wt%	water solubility wt%
25 °C dodecane	0.0052	0.0065
40 °C dodecane	0.012	0.013
40 °C mesitylene	0.053	0.052

To illustrate the generality of the MVE separation process, Fig. 11 reports concentration histories for aqueous furfural extraction into dodecane at 40 °C. Lines correspond to a priori prediction from theory. As with butanol, good agreement is evident. Whether or not a given semi-volatile solute or solute

mixture is amenable to MVE depends on favorable vapor/liquid equilibria, not membrane chemistry.

During MVE, a small amount of water can volatilize and absorb into the extracting solvent. Table 3 shows measured results for water carryover in the dodecane and mesitylene downstream solvents after solvent equilibration in the transient flow-loop experiments at 25 or 40 °C and at 40 mL/min. All measured solvent water contents are close to their saturation limits without butanol present. Although butanol partitions more favorably into mesitylene, water uptake is also higher. Thus, because the separation factor is lower for mesitylene than that for dodecane, judicious choice of solvent is important.

5. Solute recovery from extract

Solute recovery from the solvent in MVE requires an additional purification step, typically distillation. It is important to consider this secondary step when choosing an appropriate solvent for MVE. To analyze the secondary separation, we simulated distillation of butanol from the MVE downstream solvents dodecane and mesitylene using ASPEN (Aspen Technology Inc., Bedford, MA). Details are given in Appendix A.

ASPEN analysis revealed that the increased water uptake and the relatively large vapor pressure of mesitylene increases the difficulty of the distillation. Distillation from both solvents with 10 ideal stages and a reflux ratio of 2 achieved the design goal of near 95% butanol overhead recovery. However, the product stream from mesitylene distillation with the same number of stages and reflux ratio had a butanol purity of 84 wt% compared to 97 wt% in dodecane distillation. To achieve similar butanol purity, distillation from mesitylene required more stages and a higher reflux ratio compared to those for distillation from dodecane. Consequently, distillation from mesitylene suffers from larger capital and operating costs relative to those for dodecane. Thus, despite lower butanol enrichments in MVE (i.e., final butanol solvent concentrations in Figs. 4 and 6–9), dodecane is preferred over mesitylene as a receiving solvent for aqueous butanol recovery. MVE solvent choice demands consideration of the entire separation process.

Recovery of butanol from a MVE product solvent is significantly easier than that from pervaporation. Typically, pervaporation concentrates butanol from 2 wt% in the feed to 20 wt% in the permeate but also carries over a significant amount of water [18,19]. The dodecanefree or mesitylene-free product stream in MVE is 95–97 wt% butanol and 3–5 wt% water [1], significantly better than that achieved in pervaporation [18].

6. Conclusions

We confirm the feasibility of MVE for removal of aqueous butanol or furfural using the downstream organic solvents dodecane or mesitylene, at two temperatures and flow rates. First, compared to traditional distillation, energy consumption with MVE is minimal owing to essential cancellation of

the enthalpies of feed vaporization and absorption by solvent. No ancillary heat-transfer equipment is necessary. Second, flux of water across the membrane is near zero because water is almost insoluble in the receiving organic solvent. Third, because transport across the membrane occurs in the vapor phase rather than in the liquid phase, membrane-transport resistance is significantly reduced compared to that in MLE or pervaporation. Fourth, solute concentration polarization is avoided in MVE. Fifth, MVE prevents liquid-liquid contact avoiding formation of persistent emulsions.

We constructed a laboratory membrane module to extract 2-wt% aqueous butanol or 1.5-wt% furfural under countercurrent flow into dodecane or mesitylene solvent at 25 and 40 °C. Feed and solvent streams operated at 100% recycle through well-stirred reservoirs. Flow channels on each side of the membrane module were thin rectangular slits. The Versapor®200 R membrane chosen for MVE was confirmed as both hydrophobic and oleophobic. Experiments with colored dyes confirmed no liquid cross-over through the omniphobic membrane. Mass-transfer coefficients for the unfilled-channel flow geometry were determined a priori using Graetz-Lévêque analysis [1,2]. Experimental mass-transfer coefficients agree with those given in our previous publication [1]. To validate further the MVE model, we independently varied the operating temperature, semi-volatile solute, and receiving solvent. The experimental data show excellent agreement with theoretical predictions for all three operating conditions. Trends in both data and theory are as expected.

Solvent choice in MVE requires consideration of the entire separation process including downstream recovery of the solute from the extracting solvent.

Acknowledgments

The authors are grateful to the Energy Bioenergy Institute of the University of California for use of facilities and to Stefan Bauer for essential advice on chemical analyses. J. Chen acknowledges the China Scholarship Council for financial assistance during her stay at the University of California, Berkeley. D.E. Liu received partial support from Chevron Technology Corporation, Richmond, CA.

Appendix A. Distillation of butanol and water from dodecane or mesitylene

Following MVE separation, biosolute extracted into a non-volatile solvent must be recovered by a secondary purification process. We simulated distillation of water-butanol-dodecane and water-butanol-mesitylene in ASPEN using the RADFRAC distillation module (Aspen Technology Inc., Bedford, MA) with a design goal of 95% butanol recovery. Figs. A1 and A2 show the process-flow diagrams for the two solvents. Distillation from either solvent was first modeled using multicomponent correlations developed by Wilson, et al. [20,21] to determine the equilibrium number of stages and the reflux ratio. Results were substituted into the RADFRAC module. To compare separation from either solvent, reboiler heat duties were fixed at 4 kW.

Distillation feed compositions were determined by engineering-design analysis for a 1.5-m long, 30-m² membrane-area countercurrent MVE unit processing 2-wt% aqueous butanol by dodecane or mesitylene solvent at 40 °C [1]. Water and butanol concentrations entering the RADFRAC unit are larger for mesitylene than for dodecane, in agreement with the reported equilibrium compositions in Table 3. A 100 kg/h basis was selected for the feed stream.

Activity coefficients in the MVE system were determined by application of the UNIQUAC model [22–24]. Binary water/butanol, water/ dodecane, and butanol/dodecane UNIQUAC parameters were calculated from vapor/liquid and liquid/liquid equilibrium data [25]. Water/ mesitylene UNIQUAC parameters were provided by the ASPEN software. Binary interaction parameters for butanol/mesitylene were determined from the UNIFAC-group contribution method as no experimental equilibrium data were available. The same UNIQUAC interaction parameters were used in both the MVE design analysis and ASPEN distillation simulations.

To distill butanol and water from dodecane, the MVE product-solvent stream is pre-heated to 170 °C and fed to the 7th stage of a 10-stage distillation column with a total condenser and a molar reflux ratio of 2. Because dodecane is essentially non-volatile, nearly all of it is recovered in the bottoms stream. Conversely, essentially all of the butanol and water vaporize and are recovered in the distillate stream. Bottoms product is 99.95-wt% dodecane for recycle to the MVE solvent-feed stream. The composition of the overheads product stream is 97-wt% butanol, 3-wt% water, and 0.1-wt% dodecane.

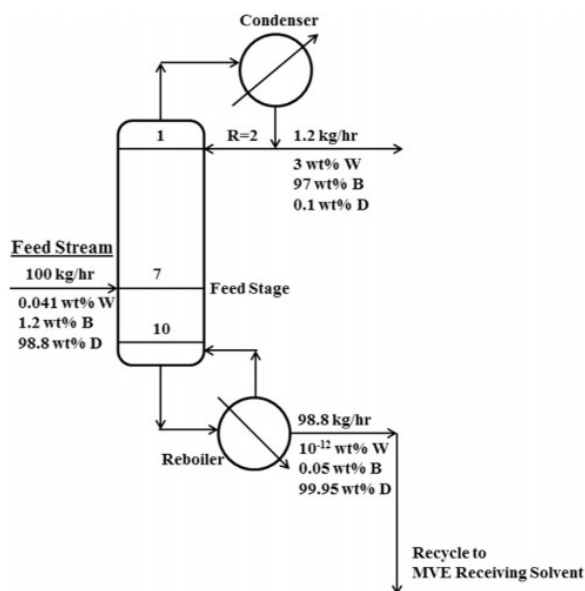


Fig. A1. Recovery of butanol from a water-butanol-dodecane MVE extract mixture by distillation. Abbreviations W, B, and D represent water, butanol, and dodecane, respectively.

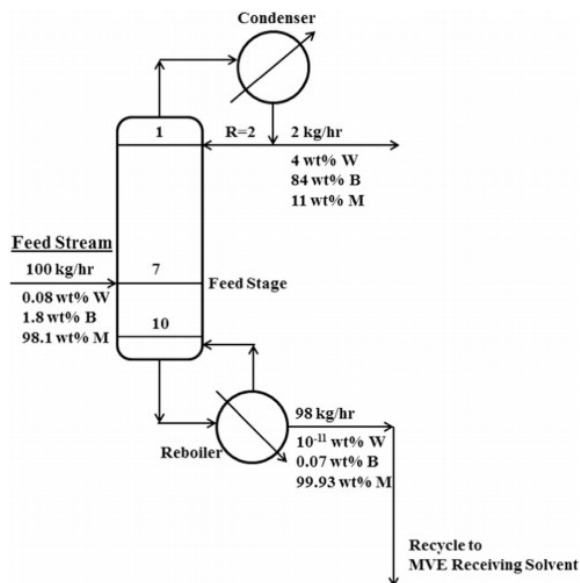


Fig. A2. Recovery of butanol from a water-butanol-mesitylene MVE extract mixture by distillation. Abbreviations W, B, and M represent water, butanol, and mesitylene, respectively.

A similar scheme was utilized for distilling butanol and water from the MVE-product mesitylene stream. Stage numbers and feed stages were the same as those for dodecane, as shown in Fig. A2, but the feed was now pre-heated to 115 °C rather than to 170 °C avoiding vaporization of mesitylene. Overall butanol recovery was now 95% and butanol purity was 84 wt%. The butanol-mesitylene distillation separation factor was 400, more than 2 orders of magnitude smaller than the butanol-dodecane separation factor of 6×10^4 . To achieve purity similar to that with dodecane, distillation of butanol from mesitylene demands more distillation stages and a higher molar reflux ratio leading to higher cost. Alternatively, a tertiary butanol recovery process may be required for further purification of the product stream from mesitylene distillation. Although mesitylene is a more favorable MVE solvent for separating butanol from water than dodecane (see Table 1), recovery of butanol from mesitylene is more difficult than that from dodecane.

References

- [1] D.E. Liu, C. Cerretani, R. Tellez, A.P. Scheer, S. Sciamanna, P.F. Bryan, C.J. Radke, J.M. Prausnitz, Analysis of countercurrent membrane vapor extraction of a dilute aqueous biosolute, *AIChE J.* 61 (2015) 2795–2809.
- [2] R.B. Bird, W.E. Stewart, E.N. Lightfoot, *Transport Phenomena*, Wiley, New York, 2002, pp. 428–432.
- [3] C.H. Park, Q.H. Geng, Simultaneous fermentation and separation in the ethanol and abe fermentation, *Sep. Purif. Methods* 21 (1992) 127–174.
- [4] D.T. Jones, D.R. Woods, Acetone-butanol fermentation revisited, *Microbiol. Rev.* 50 (1986) 484–524.
- [5] B.P. Tracy, Improving butanol fermentation to enter the advanced biofuel market, *mBio* 3 (2012).

- [6] G. Stephanopoulos, Challenges in engineering microbes for biofuels production, *Science* 315 (2007) 801–804.
- [7] A. Alkudhiri, N. Darwish, N. Hilal, Membrane distillation: a comprehensive review, *Desalination* 287 (2012) 2–18.
- [8] B.M. Kim, Membrane-based solvent extraction for selective removal and recovery of metals, *J. Membr. Sci.* 21 (1984) 5–19.
- [9] A. Dupuy, V. Athes, J. Schenk, U. Jenelten, I. Souchon, Experimental and theoretical considerations on breakthrough pressure in membrane-based solvent extraction: focus on citrus essential oil/hydro-alcoholic solvent systems with low interfacial tension, *J. Membr. Sci.* 378 (2011) 203–213.
- [10] Y.L. Hwang, G.E. Keller, J.D. Olson, Steam stripping for removal of organic pollutants from water. 1. Stripping effectiveness and stripper design, *Ind. Eng. Chem. Res* 31 (1992) 1753–1759.
- [11] Y.L. Hwang, J.D. Olson, G.E. Keller, Steam stripping for removal of organic pollutants from water. 2. Vapor-liquid-equilibrium data, *Ind. Eng. Chem. Res.* 31 (1992) 1759–1768.
- [12] M. Gryta, M.K. Karakulski, The application of membrane distillation for the concentration of oil-water emulsion, *Desalination* 121 (1991) 23–29.
- [13] A. Wang, N.P. Balsara, A.T. Bell, Pervaporation-assisted catalytic conversion of xylose to furfural, *Green. Chem.* 18 (2016) 4073–4085.
- [14] Pall Corporation, Versapor R membrane data sheet. (<https://www.pall.com/pdfs/misc/IMGVRMEN.pdf>), 2010 (accessed 21.9.16).
- [15] S.F.Y. Li, H.M. Ong, Infinite dilution diffusion-coefficients of several alcohols in water, *J. Chem. Eng. Data* 35 (1990) 136–137.
- [16] Teledyne Isco, Measurement of binary diffusion coefficients of compounds at infinite dilution in water as a function of temperature. (http://www.isco.com/WebProductFiles/Applications/105/Application_Notes/Measurement_of_Binary_Diffusion_Coefficients_as_Function_of_Temperature.pdf), 2011 (accessed 21.12.16)
- [17] D.Y. Kwok, T. Gietzelt, K. Grundke, H.J. Jacobasch, A.W. Neumann, Contact angle measurements and contact angle interpretation. 1. Contact angle measurements by axisymmetric drop shape analysis and a goniometer sessile drop technique, *Langmuir* 13 (1997) 2880–2894.
- [18] H.J. Huang, S. Ramaswamy, Y. Liu, Separation and purification of biobutanol during bioconversion of biomass, *Sep. Purif. Technol.* 132 (2014) 513–540.
- [19] N. Qureshi, H.P. Blaschek, Butanol recovery from model solution/fermentation broth by pervaporation: evaluation of membrane performance, *Biomass Bioenergy* 17 (1999) 175–184.

- [20] G.M. Wilson, C.H. Deal, activity coefficients and molecular structure. Activity coefficients in changing environments-solutions of groups, Ind. Eng. Chem. Fund. 1 (1962) 20-23.
- [21] J. Gmehling, U. Onken, Vapor-liquid equilibrium data collection: aqueous-organic systems, in: D. Behrens, R. Eckermann (Eds.) Chemistry Data Series, Frankfurt, Germany, 1977
- [22] D.S. Abrams, J.M. Prausnitz, Statistical thermodynamics of liquid mixtures: a new expression for the excess Gibbs energy of partly or completely miscible systems, AIChE J. 21 (1975) 116-128.
- [23] T.F. Anderson, J.M. Prausnitz, Application of UNIQUAC equation to calculation of multicomponent phase-equilibria. 1. vapor-liquid-equilibria, Ind. Eng. Chem. Process Des. Dev. 17 (1978) 552-561.
- [24] T.F. Anderson, J.M. Prausnitz, Application of UNIQUAC equation to calculation of multicomponent phase-equilibria. 2. Liquid-liquid equilibria, Ind. Eng. Chem. Process Des. Dev. 17 (1978) 561-567.
- [25] S. Balasubramonian, S. Kumar, D. Sivakumar, U.K. Mudali, Application of COSMORS method for the prediction of liquid-liquid equilibrium of water/n-dodecane/1- butanol, Int. Sch. Res. Not. Thermodyn. 2014 (2014) 1-6.